Pergamon

Int. J. Solids Structures Vol. 31, No. 16, pp. 2281–2297, 1994

0020–7683/94 $7.00 + .00

0020–7683(93)E0043–H

FREQUENCY AND MODE SHAPE ANALYSIS OF RESTRAINED BEAM-TYPE STRUCTURE WITH TWO INTERMEDIATE CRACKS/MASS FOR VIBRATION DIAGNOSIS

S. H. FARGHALY
Department of Mechanical Design, Faculty of Engineering and Technology, Mataria, Post Code 11718, University of Helwan, Cairo, Egypt

(*Received in final form* 28 *September* 1993)

Abstract—A mathematical model to study the influence on the system vibration modes of one or two cracks in a uniform prismatic beam elastically restrained against rotation and translation at both ends and carrying lumped masses with rotary inertia, is presented. Parametric studies are carried out for the effect of stiffness of elastic constraints, the location and magnitude of cracks, concentrated masses and their rotary inertia, for the 10 combinations of the well known four classical end conditions, on the natural frequency parameters and mode shapes of the system. A system frequency equation is derived in a discrete matrix form. Good agreement is found between the results obtained using the model presented and those of previous investigators. The typical frequency charts of the present study may be useful to engineering design and non-destructive testing analysts as a tool for diagnosis and detection of cracks in engineering applications.

1. INTRODUCTION

Strong interest has developed within the past several years in the dynamic behaviour of beams and shafts with cracks. Vibration investigation of damaged structures is one approach for fault diagnosis. Vibration diagnosis, as a non-destructive detection technique, has recently become of greater importance. An ultrasonic pulse technique has been successfully used to detect the positions of cracks in structures and welds. In some materials, this technique may not be practical due to the large attenuation of the signal at all frequencies except a particular one. Radiographic techniques have been used for crack detection in structures, and require, however, higher radiation energy input for increasing material thickness, which increases the cost of operation or equipment. Work on non-destructive testing by vibration technique has been reported by Cawly and Adams (1979).

A crack which occurs in a structural element causes some local variations in its stiffness which affect the dynamics of the whole structure to a considerable degree. The frequencies of natural vibrations, amplitude of forced vibrations, local flexibilities and areas of dynamic stability change due to the existence of such cracks have been studied by Petroski (1981), Gudmundson (1984), Christides and Barr (1984), Gounaris and Dimarogonas (1988), Shen and Pierre (1990) and Gao and Herrman (1992). An analysis of the changes makes it possible to identify the cracks without disassembly of the system. A method of analysis of the effect of two open cracks upon the frequencies of the natural flexural vibrations in a cantilever beam is presented by Ostachowicz and Krawczuk (1991). Two types of cracks—single sided and double sided—are considered, assuming that the cracks occur in the first mode of fracture, i.e. the opening mode. The influence of the slenderness ratio of a stationary shaft with an open crack on the dynamic behaviour of the beam was investigated by Kikidis and Papadopoulos (1992). Their results were obtained by using the Euler–Bernoulli theory and compared with those from the Timoshenko theory. The natural vibrations of a cracked stationary shaft system, that is a continuous cracked shaft with elastically mounted end mass, is investigated by El-Dannanh and Farghaly (1994).

An exact approach is extensively used to analyse the vibrations of beams carrying intermediate masses. In this approach the frequency and mode shape equations may be

derived by dividing the beam into segments at each point of which the beam has an intermediate concentrated element. One then formulates the equation of motion for each segment, and needs the solution to each of these equations to satisfy all the boundary conditions and the continuity conditions at the ends of the particular segment. Many authors have used this approach to study the free and forced vibrations of beams carrying concentrated masses and/or elastic supports at intermediate points with various boundary conditions. For this, only selected references are given. Srinath and Das (1967) studied the fundamental eigenfrequencies of a simply supported uniform beam carrying an arbitrary located mass having rotary inertia. Liu and Huang (1988) determined the first five eigenfrequencies of a uniform cantilever beam restrained against rotation at its base, and with an intermediate translational and rotational elastic constraint, and carrying a heavy load at its tip. The application of this approach to the solution of a beam problem with intermediate concentrated elements at n different points involves the solution of n simultaneous boundary value problems, and the solution generally gives a complicated characteristics equation. Bapat and Bapat (1987) used this approach together with the transfer matrix method to treat the free vibrations of a uniform beam having any number of intermediate point masses and elastic supports. Numerical study of the convergence characteristics and accuracies of three approximate discretization methods, Rayleigh–Ritz, Galerkin, and finite element as applied to the analysis of linear bending free vibrations of cantilever beam carrying a mass with rotary inertia at the free end and another at an intermediate point, has been presented by Hamdan and Abd-El Latif (1992). An anlytical study of a system of elastically supported multi-span stepped uniform beams has been presented by Farghaly (1994). The beam was loaded at the end as well as at intermediate points with inertial and elastic elements. Exact natural frequencies were obtained for uniform and stepped beams with three or two spans.

Although researchers have focused on beam systems with concentrated masses or cracks, no one (to the best of the author's knowledge), has completely treated the combined problem as presented in the following investigation in which parametric studies are carried out for the effect of the stiffness of the elastic constraints, the location and magnitude of the cracks, the concentrated masses and their rotary inertia, for the 10 combinations of the classical end conditions, on the natural frequency parameters and mode shapes of the system. The results of this investigation are compared with existing published results. For convenience, all results are presented in dimensionless form. Ostachowicz and Krawczuk recent flexibility polynomials are used in the formulation of the problem. Also, derivation of the characteristic equation is based on Euler–Bernoulli beam bending theory and consequently a simple algorithm is to be used to solve this equation. However, it is believed that the results of this study may be useful to engineering design and non-destructive testing analysts as a tool for diagnosis and detection of cracks in engineering applications.

2. ANALYSIS

2.1. *Elastic behaviour of a cracked beam*

The crack flexibility depends on the crack orientation and magnitude with respect to the main dimensions of the cracked member and on the applied loadings and the mode of deformation. In the following, the cracks are assumed to occur in the first mode of fracture: i.e. the opening mode. The non-dimensional local flexibility of the double-sided cracked section of equal depth (Ostachowicz and Krawczuk, 1991; Alturi, 1986; Haisty and Springer, 1988), may be written in the form

$$\theta_{DS} = 6\pi\gamma^2\bar{h}f_D(\gamma) \tag{1}$$

where

$$f_D(\gamma) = 0.5335 - 0.929\gamma + 3.500\gamma^2 - 3.181\gamma^3 + 5.793\gamma^4$$

and

$$\gamma = d/h; \qquad \bar{h} = h/L.$$

On the other hand, the equivalent flexibility at the location of the single-sided crack is formulated as used in Gudmundson (1984) and Ostachowicz (1991), and its non-dimensional form may be written as:

$$\theta_S = 6\pi\gamma^2\bar{h}f_S(\gamma) \tag{2}$$

where

$$f_S(\gamma) = 0.6384 - 1.035\gamma + 3.7201\gamma^2 - 5.1773\gamma^3 + 7.553\gamma^4 - 7.332\gamma^5 + 2.4909\gamma^6.$$

2.2. *Cracked beam mode*

The crack is assumed to be open and to have uniform depth. It is known that the modes of harmonic vibration on the three segments of the beam system shown in Fig. 1, in non-dimensional form (Bishop and Johnson, 1979), are:

$$Y_1(\zeta_1) = A_1 \sin\beta\zeta_1 + A_2\cos\beta\zeta_1 + A_3\sinh\beta\zeta_1 + A_4\cosh\beta\zeta_1 \tag{3a}$$

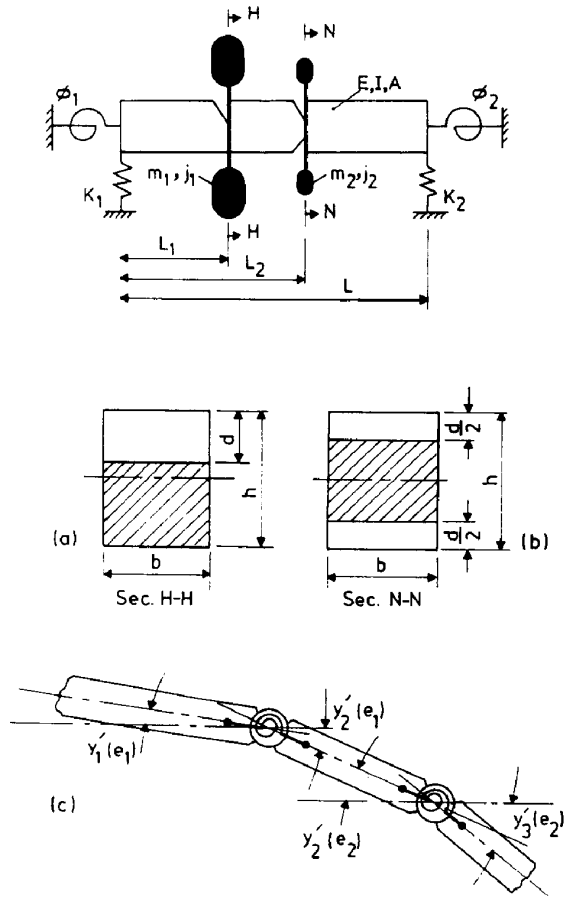

Fig. 1. Elastically restrained beam with two cracks and intermediate concentrated masses: (a) single-sided crack section; (b) double-sided crack section; and (c) crack model and the system co-ordinates.

$$Y_2(\zeta_2) = A_5 \sin \beta\zeta_2 + A_6 \cos \beta\zeta_2 + A_7 \sinh \beta\zeta_2 + A_8 \cosh \beta\zeta_2 \tag{3b}$$

$$Y_3(\zeta_3) = A_9 \sin \beta\zeta_3 + A_{10} \cos \beta\zeta_3 + A_{11} \sinh \beta\zeta_3 + A_{12} \cosh \beta\zeta_3 \tag{3c}$$

where Y_1, Y_2 and Y_3 are the solutions of the polynomial of the system equation of motion

$$Y_i''''(\zeta_i) - \beta^4 Y_i(\zeta_i) = 0, \qquad i = 1, 2, 3.$$

This is the well known fourth order Euler–Bernoulli equation of motion for beams vibrating in the bending mode. In equations (3), A_1, A_2, ..., and A_{12}, are unknown coefficients to be determined from the boundary, continuity and compatibility conditions, $\beta^4 = \rho A L^4 \Omega^2 / EI$, Ω is the circular frequency, ρ is the beam material density, A is the cross-sectional area and $\zeta_i = x_i/L$, where x_i is the co-ordinate along the beam for the ith segment. If the unknown coefficients are obtained, the system mode shape can be determined.

2.3. *Application to the present model*

The model presented is a uniform beam elastically restrained against rotation and translation at each end, and carrying lumped masses with rotary inertia at two arbitrary intermediate points whose local flexibility may be reduced to the existence of open cracks. The boundary conditions are

at $\zeta = 0$

$$Y_1'(0) - \Phi_1 Y_1(0) = 0; \tag{4a}$$

$$Y_1'''(0) + Z_1 Y_1(0) = 0 \tag{4b}$$

at $\zeta = 1$:

$$Y_3'(1) + \Phi_2 Y_3(1) = 0; \tag{4c}$$

$$Y_3'''(1) - Z_2 Y_3(1) = 0 \tag{4d}$$

here, $\Phi_i = \phi_i L/EI$; and $Z_i = K_i L^3/EI$; $i = 1, 2$, are the rotational and the translational rigidity parameters of the ends respectively. If $e_1 = L_1/L$ and $e_2 = L_2/L$ are the non-dimensional crack positions, the continuity conditions at these positions are

at $\zeta = e_1$:

$$Y_1(e_1) - Y_2(e_1) = 0 \tag{5a}$$

$$Y_1'(e_1) - Y_2'(e_1) - \bar{J}_1 \beta^4 Y_1(e_1) = 0 \tag{5b}$$

$$Y_1'''(e_1) - Y_2'''(e_1) + \bar{m}_1 \beta^4 Y_2(e_1) = 0 \tag{5c}$$

at $\zeta = e_2$:

$$Y_2(e_2) - Y_3(e_2) = 0 \tag{5d}$$

$$Y_2'(e_2) - Y_3'(e_2) - \bar{J}_2 \beta^4 Y_2'(e_2) = 0 \tag{5e}$$

$$Y_2'''(e_2) - Y_3'''(e_2) + \bar{m}_2 \beta^4 Y_3(e_2) = 0 \tag{5f}$$

here

$$\bar{J}_i = J_i/(\rho A L^3); \qquad \bar{m}_i = m_i/m; \qquad i = 1, 2$$

and the compatibility conditions due to rotational flexibility at the crack location are

at $\zeta = e_1$:

$$Y_2'(e_1) - Y_1'(e_1) - \theta_1 Y_2''(e_1) = 0 \tag{6a}$$

at $\zeta = e_2$:
$$Y_3'(e_2) - Y_2'(e_2) - \theta_2 Y_3''(e_2) = 0. \qquad (6b)$$

For single-sided cracks, $\theta_i = 6\pi\gamma_i^2\bar{h}f_S(\gamma_i)$, $i = 1, 2$, and for double-sided cracks, $\theta_i = 6\pi\gamma_i^2\bar{h}f_D(\gamma_i)$, $i = 1, 2$. Combination of eqns (3) with eqns (4–6) yields the characteristic equation (7) which in turn gives the natural frequencies:

$$\det([FF] + [CM] + [ES] + [CR]) = 0 \qquad (7)$$

where $[FF]$ is a matrix 12×12 for a free–free beam, $[CM]$ is a matrix representing the lumped masses and their rotary inertia, $[ES]$ is a matrix of the end rigidity parameters, while $[CR]$ is a matrix representing the local crack flexibility elements. These matrices may be written in a proposed discrete form as

$$[FF] = \begin{bmatrix} 0 & -\beta & 0 & \beta & 0 & 0 & 0 & 0 & 0 & 0 & 0 & 0 \\ -\beta^3 & 0 & \beta^3 & 0 & 0 & 0 & 0 & 0 & 0 & 0 & 0 & 0 \\ sa_1 & ca_1 & sha_1 & cha_1 & -sa_1 & -ca_1 & -sha_1 & -cha_1 & 0 & 0 & 0 & 0 \\ ca_1 & -sa_1 & cha_1 & sha_1 & -ca_1 & sa_1 & -cha_1 & -sha_1 & 0 & 0 & 0 & 0 \\ -sa_1 & -ca_1 & sha_1 & cha_1 & sa_1 & ca_1 & -sha_1 & -cha_1 & 0 & 0 & 0 & 0 \\ -ca_1 & sa_1 & cha_1 & sha_1 & ca_1 & -sa_1 & -cha_1 & -sha_1 & 0 & 0 & 0 & 0 \\ 0 & 0 & 0 & 0 & sa_2 & ca_2 & sha_2 & cha_2 & -sa_2 & -ca_2 & -sha_2 & -cha_2 \\ 0 & 0 & 0 & 0 & ca_2 & -sa_2 & cha_2 & sha_2 & -ca_2 & sa_2 & -cha_2 & -sha_2 \\ 0 & 0 & 0 & 0 & -sa_2 & -ca_2 & sha_2 & cha_2 & sa_2 & ca_2 & -sha_2 & -cha_2 \\ 0 & 0 & 0 & 0 & -ca_2 & sa_2 & cha_2 & sha_2 & ca_2 & -sa_2 & -cha_2 & -sha_2 \\ 0 & 0 & 0 & 0 & 0 & 0 & 0 & 0 & -\beta s\beta & -\beta c\beta & \beta sh\beta & \beta ch\beta \\ 0 & 0 & 0 & 0 & 0 & 0 & 0 & 0 & -\beta^3 c\beta & \beta^3 s\beta & \beta^3 ch\beta & \beta^3 sh\beta \end{bmatrix}$$

$$[ES] = \begin{bmatrix} -\Phi_1 & 0 & -\Phi_1 & 0 & 0 & 0 & 0 & 0 & 0 & 0 & 0 & 0 \\ 0 & Z_1 & 0 & Z_1 & 0 & 0 & 0 & 0 & 0 & 0 & 0 & 0 \\ 0 & 0 & 0 & 0 & 0 & 0 & 0 & 0 & 0 & 0 & 0 & 0 \\ 0 & 0 & 0 & 0 & 0 & 0 & 0 & 0 & 0 & 0 & 0 & 0 \\ 0 & 0 & 0 & 0 & 0 & 0 & 0 & 0 & 0 & 0 & 0 & 0 \\ 0 & 0 & 0 & 0 & 0 & 0 & 0 & 0 & 0 & 0 & 0 & 0 \\ 0 & 0 & 0 & 0 & 0 & 0 & 0 & 0 & 0 & 0 & 0 & 0 \\ 0 & 0 & 0 & 0 & 0 & 0 & 0 & 0 & 0 & 0 & 0 & 0 \\ 0 & 0 & 0 & 0 & 0 & 0 & 0 & 0 & 0 & 0 & 0 & 0 \\ 0 & 0 & 0 & 0 & 0 & 0 & 0 & 0 & 0 & 0 & 0 & 0 \\ 0 & 0 & 0 & 0 & 0 & 0 & 0 & 0 & \Phi_2 c\beta & -\Phi_2 s\beta & \Phi_2 ch\beta & \Phi_2 sh\beta \\ 0 & 0 & 0 & 0 & 0 & 0 & 0 & 0 & -Z_2 s\beta & -Z_2 c\beta & -Z_2 sh\beta & -Z_2 ch\beta \end{bmatrix}$$

$$[CM] = \begin{bmatrix} 0 & 0 & 0 & 0 & 0 & 0 \\ 0 & 0 & 0 & 0 & 0 & 0 \\ 0 & 0 & 0 & 0 & 0 & 0 \\ 0 & 0 & 0 & 0 & 0 & 0 \\ -\bar{J}_1\beta^3 ca_1 & -\bar{J}_1\beta^3 sa_1 & -\bar{J}_1\beta^3 cha_1 & -\bar{J}_1\beta^3 sha_1 & 0 & 0 \\ 0 & 0 & 0 & 0 & \bar{m}_1\beta sa_1 & \bar{m}_1\beta ca_1 \\ 0 & 0 & 0 & 0 & 0 & 0 \\ 0 & 0 & 0 & 0 & 0 & 0 \\ 0 & 0 & 0 & 0 & -\bar{J}_2\beta^3 ca_2 & \bar{J}_2\beta^3 sa_2 \\ 0 & 0 & 0 & 0 & 0 & 0 \\ 0 & 0 & 0 & 0 & 0 & 0 \\ 0 & 0 & 0 & 0 & 0 & 0 \end{bmatrix}$$

$$\begin{bmatrix} 0 & 0 & 0 & 0 & 0 & 0 \\ 0 & 0 & 0 & 0 & 0 & 0 \\ 0 & 0 & 0 & 0 & 0 & 0 \\ 0 & 0 & 0 & 0 & 0 & 0 \\ 0 & 0 & 0 & 0 & 0 & 0 \\ \bar{m}_1\beta sha_1 & \bar{m}_1\beta cha_1 & 0 & 0 & 0 & 0 \\ 0 & 0 & 0 & 0 & 0 & 0 \\ 0 & 0 & 0 & 0 & 0 & 0 \\ -\bar{J}_2\beta^3 cha_2 & -\bar{J}_2\beta^3 sha_2 & 0 & 0 & 0 & 0 \\ 0 & 0 & \bar{m}_2\beta sa_2 & \bar{m}_2\beta ca_2 & \bar{m}_2\beta sha_2 & \bar{m}_2\beta cha_2 \\ 0 & 0 & 0 & 0 & 0 & 0 \\ 0 & 0 & 0 & 0 & 0 & 0 \end{bmatrix}$$

$$[CR] = \begin{bmatrix} 0 & 0 & 0 & 0 & 0 & 0 \\ 0 & 0 & 0 & 0 & 0 & 0 \\ 0 & 0 & 0 & 0 & 0 & 0 \\ 0 & 0 & 0 & 0 & -v_1 sa_1 & -v_1 ca_1 \\ 0 & 0 & 0 & 0 & 0 & 0 \\ 0 & 0 & 0 & 0 & 0 & 0 \\ 0 & 0 & 0 & 0 & 0 & 0 \\ 0 & 0 & 0 & 0 & 0 & 0 \\ 0 & 0 & 0 & 0 & 0 & 0 \\ 0 & 0 & 0 & 0 & 0 & 0 \\ 0 & 0 & 0 & 0 & 0 & 0 \end{bmatrix}$$

$$\begin{bmatrix} 0 & 0 & 0 & 0 & 0 & 0 \\ 0 & 0 & 0 & 0 & 0 & 0 \\ 0 & 0 & 0 & 0 & 0 & 0 \\ v_1 sha_1 & v_1 cha_1 & 0 & 0 & 0 & 0 \\ 0 & 0 & 0 & 0 & 0 & 0 \\ 0 & 0 & 0 & 0 & 0 & 0 \\ 0 & 0 & 0 & 0 & 0 & 0 \\ 0 & 0 & -v_2 sa_2 & -v_2 ca_2 & v_2 sha_2 & v_2 cha_2 \\ 0 & 0 & 0 & 0 & 0 & 0 \\ 0 & 0 & 0 & 0 & 0 & 0 \\ 0 & 0 & 0 & 0 & 0 & 0 \\ 0 & 0 & 0 & 0 & 0 & 0 \end{bmatrix}$$

where

$$a_1 = e_1\beta; \qquad a_2 = e_2\beta; \qquad v_1 = \theta_1\beta; \qquad v_2 = \theta_2\beta;$$

$sh(\ ) \triangleq \sinh(\ )$; $ch(\ ) \triangleq \cosh(\ )$; $s(\ ) \triangleq \sin(\ )$; and $c(\ ) \triangleq \cos(\ )$.

3. APPLICATIONS AND RESULTS

3.1. *Natural frequency and mode shape results*

3.1.1. *Comparison with previous results.* To check the validity of characteristic eqn (7), two examples are chosen. The first is a cantilever beam, having two different cracks of depth parameters $\gamma_1 = 0.5$ and $\gamma_2 = 0.3$ located at $\zeta = 0.1$ and $\zeta = 0.2$ respectively (Ostachowicz and Krawczuk, 1991) while the second example is a cantilever beam, carrying two inertia elements located at $e_1 = 0.5$ and $e_2 = 1.0$ and having $\bar{m}_1 = \bar{J}_1 = 0.1$ and $\bar{m}_2 = \bar{J}_2 = 0.1$ respectively (Hamdan and Abd-El Latif, 1992). To obtain the numerical results two computer programs were developed and then run using FORTRAN 77 and PC-MATLAB software on an AMSTRAD PC286, the false position technique being used to bracket the system roots (eigenvalues or frequency parameters). The results have been computed taking into account the effect of all design parameters: crack and mass location parameters e_1 and e_2; crack depth parameters γ_1 and γ_2; slenderness ratio $\bar{s}$; intermediate mass parameters $\bar{m}_1$ and $\bar{m}_2$; and the end rigidity parameters Φ_1, Z_1, Φ_2 and Z_2. Table 1 shows that the results obtained using derived equation (7) and those of previous investigators are in good agreement.

For the examples 1 and 2 depicted in Table 1, the five mode shapes are plotted in Fig. 2. For example 1, Fig. 2(a) shows a discontinuity in the slope that appears at the crack locations if they exist around the points in which the respective curvatures reach the highest values corresponding to the higher mode shapes. Also, if the crack is close to a nodal point, the mode shape is unaffected by the crack, even for high values of depth. The changes in the local slope due to cracks may be significant for the higher modes, in agreement with reports by Shen and Pierre (1990); this may depend on the system end conditions and the relative crack locations with respect to the nodal points. It is interesting to note that to estimate a crack position and depth from vibration measurement, both the modal frequency and mode shape are needed.

Table 1. Comparison of present results with those of previous works: Ostachowicz (1991) and Hamdan (1992)

	Example 1		Example 2	
Design parameters	Ostachowicz (1991)	Present	Hamdan (1992)	Present
Crack parameters				
e_1	0.1	0.1	0.5	0.5
e_2	0.2	0.2	1.0	1.0
γ_1	0.5	0.5	—	*VS*
γ_2	0.3	0.3	—	*VS*
$\bar{h}$	0.1	0.1	—	*VS*
Mass parameters				
$\bar{m}_1$	—	*VS*	0.1	0.1
$\bar{m}_2$	—	*VS*	0.1	0.1
$\bar{J}_1$	—	*VS*	0.1	0.1
$\bar{J}_2$	—	*VS*	0.1	0.1
Rigidity parameters				
Φ_1	—	*VL*	—	*VL*
Z_1	—	*VL*	—	*VL*
Φ_2	—	*VS*	—	*VS*
Z_2	—	*VS*	—	*VS*
The output first five frequency parameters				
β_1	1.5452	1.545192	1.433977	1.433977
β_2	—	4.496557	2.437469	2.437468
β_3	—	7.648008	3.843954	3.843953
β_4	—	10.655835	5.361086	5.361085
β_5	—	13.737517	9.811747	9.811732

— Not included, $VS = 0.00000001$, $VL = 100000000$.

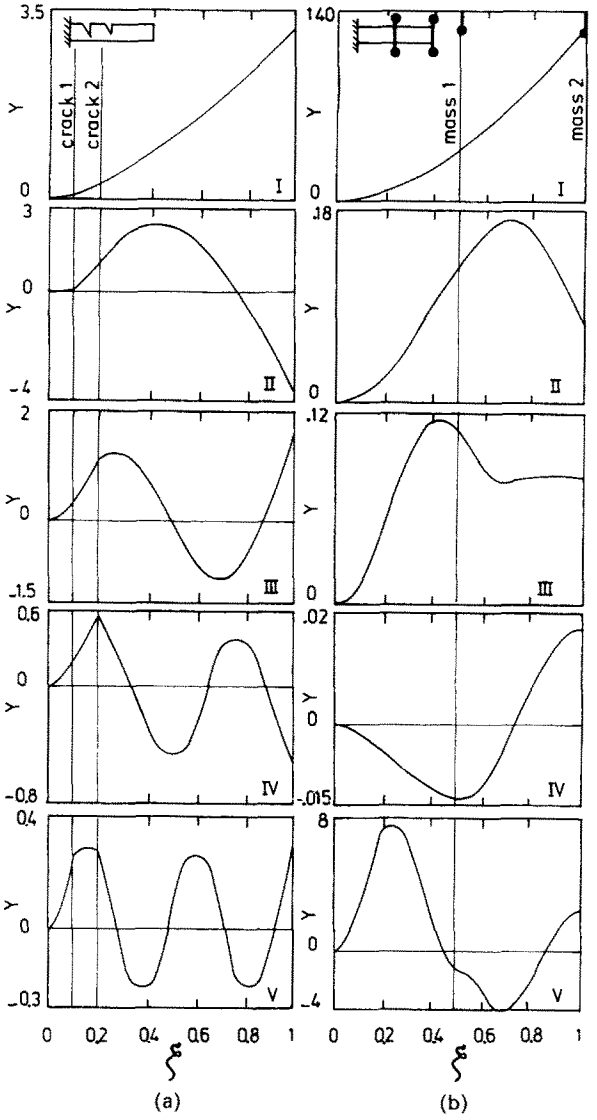

Fig. 2. The first mode shapes for the results depicted in Table 1, (a) example 1, and (b) example 2.

The effect of the concentrated masses and their rotary inertia (example 2) on the mode shapes is illustrated in Fig. 2(b). It can be seen from this figure that, for the inertia elements considered, the node of the second and the third mode disappeared as in the first mode, while the fourth mode became similar to the second mode, etc. One can obtain easily the system mode shapes for the 10 cases plotted in Figs 3–13. It is interesting to note that, for more than one crack in a beam, the first five modes may be required for the crack detection.

3.1.2. *Continuous systems with crack located at the same point of the concentrated mass* m_1. Four of the classical end conditions are combined into 10 cases using the two extreme values of the end rigidity parameters ($VS = 0.00000001$, and $VL = 100000000$, corresponding to 0 and ∞) respectively. All results are presented in terms of modal frequency ratio Ω_i—the ratio of the cracked beam frequency to that of the uncracked beam (see Table 2 for details), and the crack location parameter ζ—the ratio of the crack location co-ordinate to the beam length L. The effect of a crack whose location can take any position along the beam length with and without lumped mass on the lower two frequencies is shown in Figs 3–12. The concentrated mass together with the crack are moved from $\zeta = 0.1$ to $\zeta = 0.9$ along the beam length. Three different crack depth parameters are chosen: $\gamma_1 = VS$, $\gamma_1 = 0.3$ and $\gamma_1 = 0.6$. The results are obtained for five different mass parameters: $\bar{m}_1 = VS$;

Table 2. Frequency values $\omega_i = \beta_{iu}^2$ for uncracked beams and for various classical end conditions (Bishop and Johnson, 1979)

End conditions	Frequency values		
	Mode I	Mode II	Mode III
Clamped–free	3.51602	22.0345	61.6972
Clamped–clamped and free–free	22.3733	61.6728	120.903
Clamped–pinned and pinned–free	15.4182	49.9649	104.248
Pinned–slide	$(\pi/2)^2$	$(3\pi/2)^2$	$(5\pi/2)^2$
Pinned–pinned and slide–slide	π^2	$(2\pi)^2$	$(3\pi)^2$
Clamped–slide and slide–free	5.59332	30.2258	74.6389

0.5; 1.0; 2.0; and 4.0. It can be seen from the curves in these figures that as the values of the crack depth and the mass parameter increase, the value of the eigenfrequency ratio Ω_i ($i = 1, 2$) decreases gradually from the left group of Figs 3–12 to the right one, as may be expected. For beam configuration in which the slope due to bending together with the lateral movement, at one or two of the beam ends, are not allowed, the natural frequency

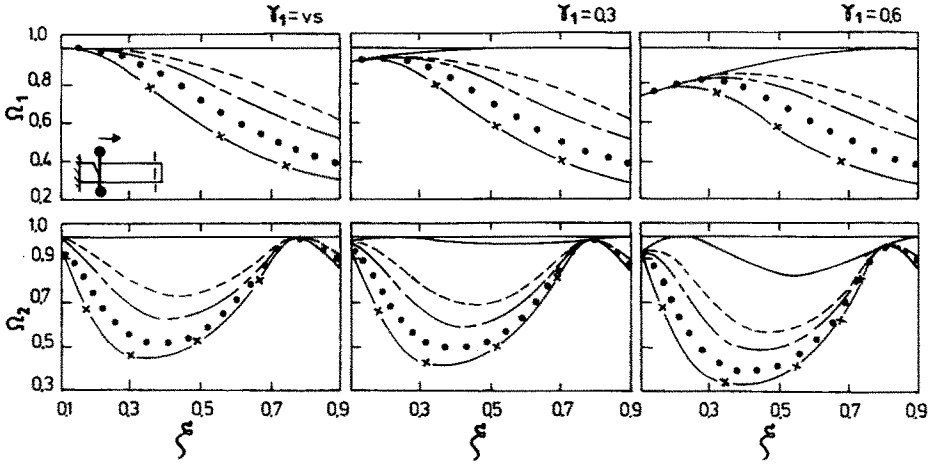

Fig. 3. Effect of the variation in the crack and mass location for the first two natural frequency ratios Ω_1 and Ω_2 for a clamped–free beam: $\bar{m}_1 = VS$, ——; $\bar{m}_1 = 0.5$, – – –; $\bar{m}_1 = 1$, ——— ; $\bar{m}_1 = 2$, ●●●●; $\bar{m}_1 = 4$, —×—.

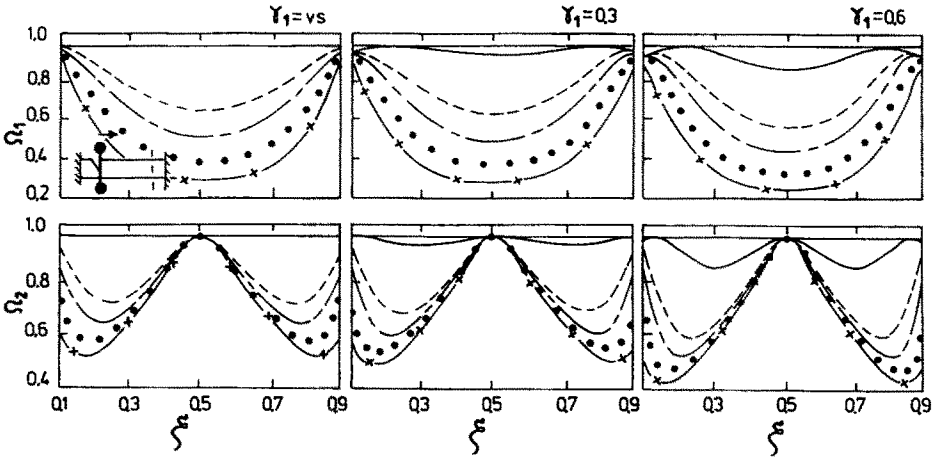

Fig. 4. Effect of the variation in the crack and mass location for the first two natural frequency ratios Ω_1 and Ω_2 for a clamped–clamped beam. Key as Fig. 3.

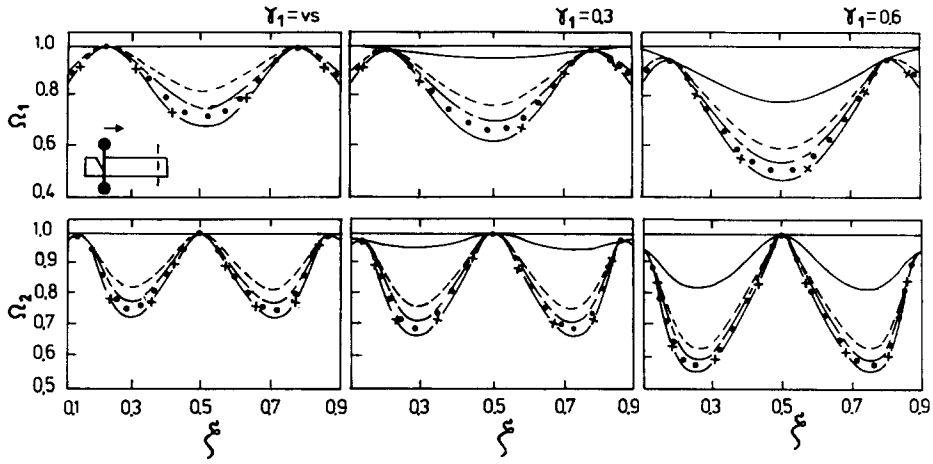

Fig. 5. Effect of the variation in the crack and mass location for the first two natural frequency ratios Ω_1 and Ω_2 for a free–free beam. Key as Fig. 3.

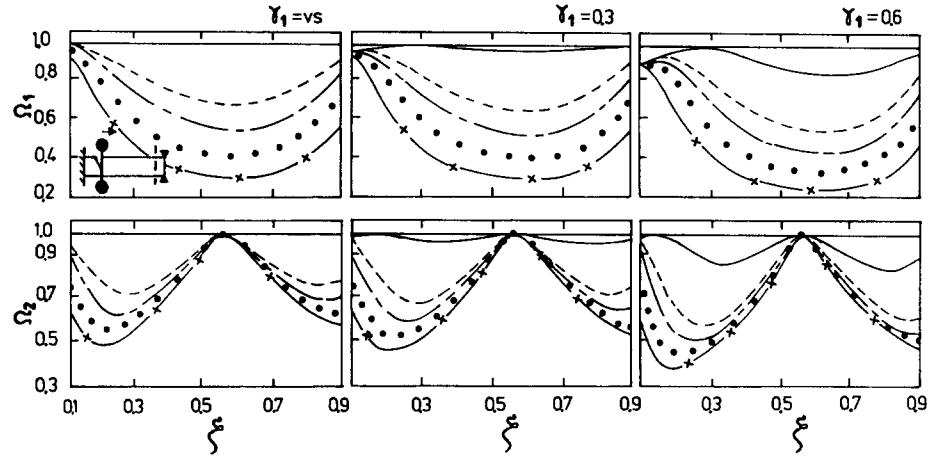

Fig. 6. Effect of the variation in the crack and mass location for the first two natural frequency ratios Ω_1 and Ω_2 for a clamped–pinned beam. Key as Fig. 3.

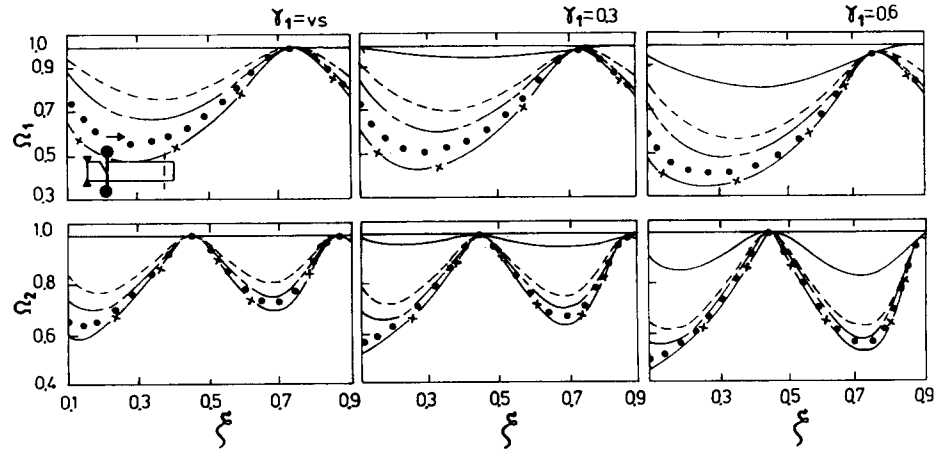

Fig. 7. Effect of the variation in the crack and mass location for the first two natural frequency ratios Ω_1 and Ω_2 for a pinned–free beam. Key as Fig. 3.

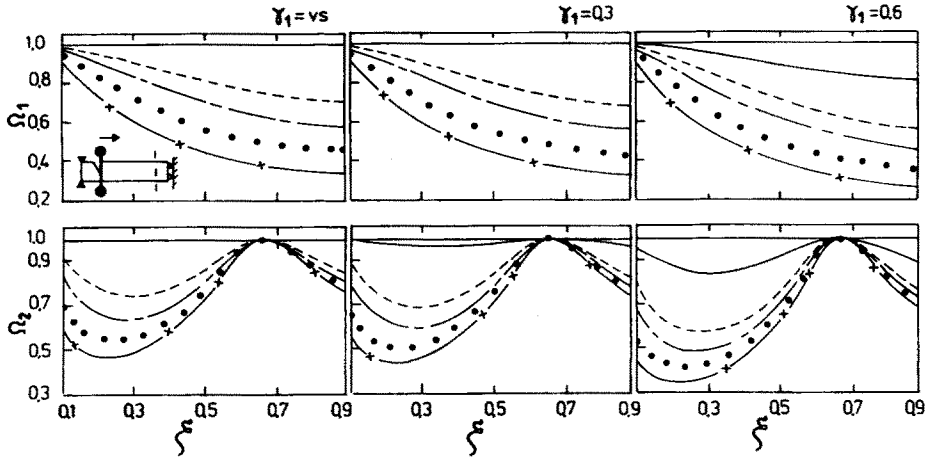

Fig. 8. Effect of the variation in the crack and mass location for the first two natural frequency ratios Ω_1 and Ω_2 for a pinned–slide beam. Key as Fig. 3.

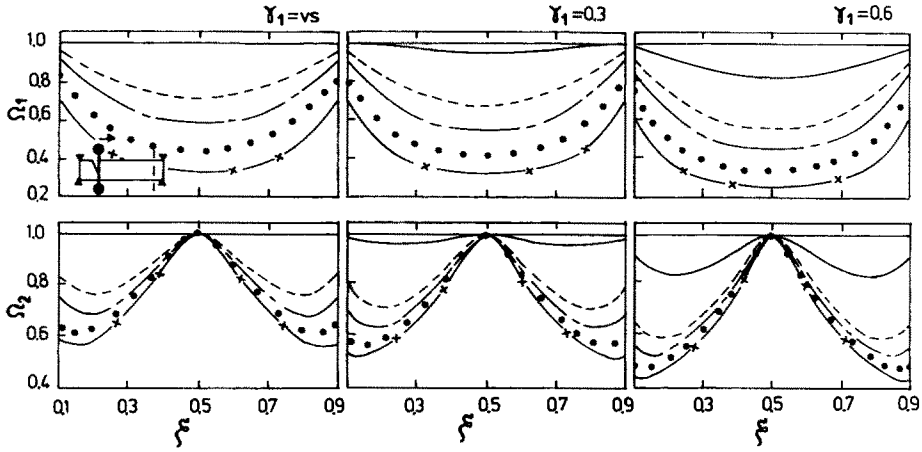

Fig. 9. Effect of the variation in the crack and mass location for the first two natural frequency ratios Ω_1 and Ω_2 for a pinned–pinned beam. Key as Fig. 3.

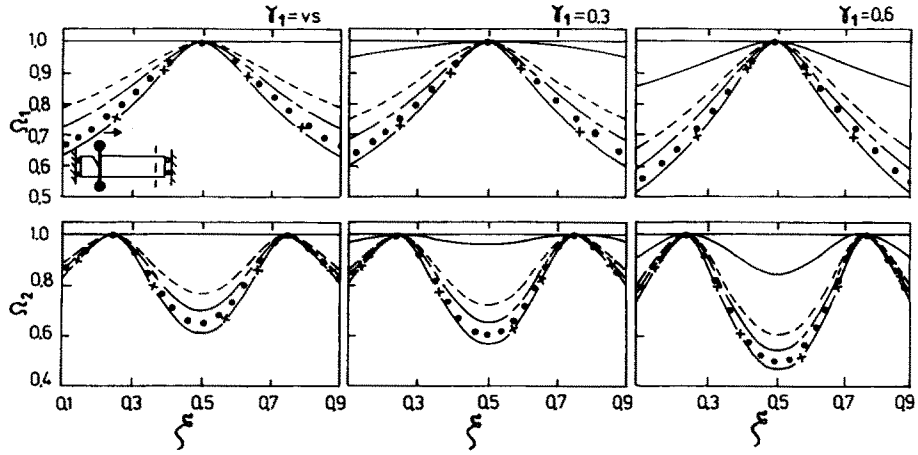

Fig. 10. Effect of the variation in the crack and mass location for the first two natural frequency ratios Ω_1 and Ω_2 for a slide–slide beam. Key as Fig. 3.

remains unaffected, at some points, by cracks and/or the masses of various values (even large). This may be due to vanishing bending moment at these points. These points are well known as the nodal points. On the contrary, the effect of the cracks together with the mass becomes dangerous at some other points in which the modal bending moment reaches its maximum value. Interesting points are observed in which the increase in the crack depth decreases the system's natural frequency, while the frequency itself is unaffected by the variation in the associated mass. This is observed only if one or two of the system end conditions become free (i.e. $Z_1 = \Phi_1 = 0$ and/or $Z_2 = \Phi_2 = 0$). For small crack depths $\gamma_1 < 0.3$, slight reduction in the frequencies is observed, meaning that frequencies have little sensitivity to the presence of small cracks.

3.1.3. *Continuous systems with crack not located at the same point of the concentrated mass* m_1. The effect of a crack not coinciding with the mass on the fundamental frequency of the system is computed for the 10 combinations of the well known classical end conditions. Five crack depth parameters: $\gamma_2 = VS$; 0.2; 0.4; 0.6; and 0.8 are chosen for this application. The results are obtained considering $\bar{m}_1 = 1$ located at $e_1 = 1/3$. Figure 13 shows the variation in the system fundamental frequency due to the variation in crack depths along the beam length (from $\zeta = 0.1$ to $\zeta = 0.9$). In general, as can be seen from these figures, an

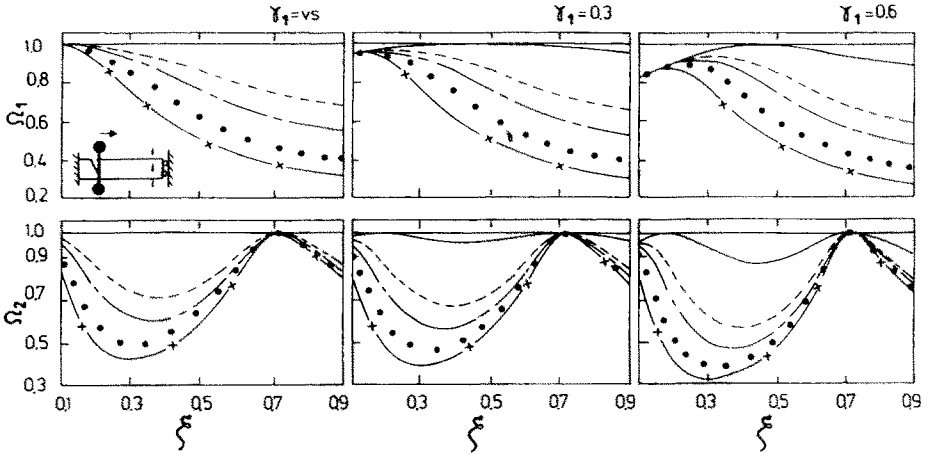

Fig. 11. Effect of the variation in the crack and mass location for the first two natural frequency ratios Ω_1 and Ω_2 for a clamped–slide beam. Key as Fig. 3.

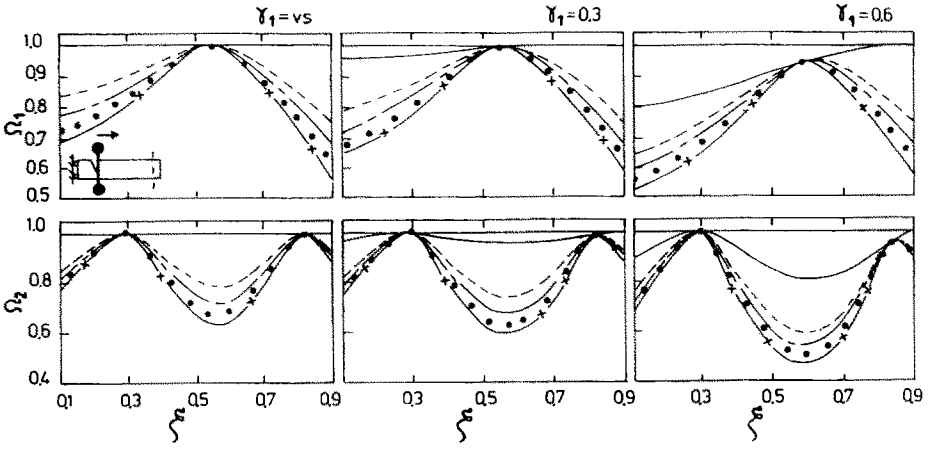

Fig. 12. Effect of the variation in the crack and mass location for the first two natural frequency ratios Ω_1 and Ω_2 for a slide–free beam. Key as Fig. 3.

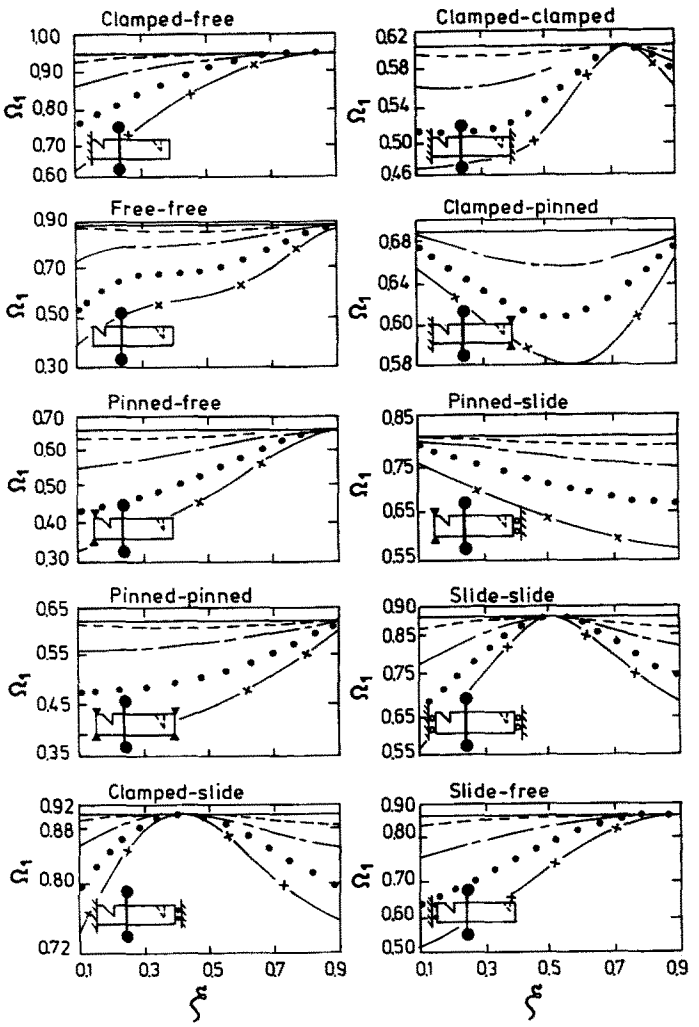

Fig. 13. Effect of the variation in the crack location and depth on the first natural frequency ratio Ω_1. $\gamma_2 = VS$, ——; $\gamma_2 = 0.2$, – – –; $\gamma_3 = 0.4$, —— – ——; $\gamma_2 = 0.6$, ●●●; $\gamma_2 = 0.8$, —×—; for the 10 combinations of the four classical end conditions.

increase in the crack depth decreases the system's natural frequency, except some points in which the crack is unaffected at this frequency. The crack becomes dangerous at certain points along the beam length, depending on the respective modal bending moment.

3.1.4. *Single-sided and double-sided cracked system.* An application example of a clamped-free beam loaded with an end mass of $\bar{m}_2 = 0.5$ and three values of mass rotary inertia, $\bar{J}_2 = vs$, 0.01 and 0.1, are considered. Three crack locations, $e_1 = 0.2$, 0.4, and 0.6, each having the relative crack depths, $\gamma_1 = vs$, 0.3 and 0.6, respectively. The first three frequency ratios $\Omega_i = (\beta_i/\beta_{iu})^2$ are obtained for the single-sided and double-sided cracked cross-section of equal depth and the results are shown in Table 3. As can be seen from this table, the double-sided cracks affect the vibration frequencies to differences not exceeding 10% from that of single-sided cracks of the same relative depth and location. Ostachowicz and Krawczuk (1991) have stated that the differences are not very large; however, they obtained results for the first mode of vibration only. Also, one can observe that an increase in the end mass rotary inertia decreases the system's natural frequencies.

3.2. *Slenderness ratio effect*

The results obtained in example 1 of Table 1 are recomputed for the slenderness ratio $\bar{s} > 10$. The change in frequency ratio for the same data for the chosen application of this

Table 3. The differences between the first three modes of single-sided (ss) and double-sided (ds) cracked cross-section for cantilever beam with end mass and rotary inertia

e_1	γ_1	$\bar{J}_2$		I	II	III
0.20E+00	0.10E−08	*vs*	ss	0.57909	0.78087	0.85552
			ds	0.57909	0.78087	0.85552
		0.01	ss	0.57073	0.61625	0.53146
			ds	0.57073	0.61625	0.53146
		0.10	ss	0.50396	0.29425	0.42433
			ds	0.50396	0.29425	0.42433
	0.30E+00	*vs*	ss	0.53024	0.77692	0.84582
			ds	0.53313	0.77715	0.84385
		0.01	ss	0.52299	0.61222	0.53128
			ds	0.52582	0.61245	0.53132
		0.10	ss	0.46505	0.29044	0.42429
			ds	0.46732	0.29065	0.42429
	0.60E+00	*vs*	ss	0.40582	0.76846	0.80725
			ds	0.34826	0.76540	0.79650
		0.01	ss	0.40089	0.60377	0.53004
			ds	0.34427	0.60070	0.52990
		0.10	ss	0.36168	0.28263	0.42422
			ds	0.31216	0.27990	0.42422
0.40E+00	0.30E+00	*vs*	ss	0.55286	0.75329	0.80636
			ds	0.55447	0.75488	0.81219
		0.01	ss	0.54462	0.60499	0.50732
			ds	0.54622	0.60566	0.50898
		0.10	ss	0.47966	0.29369	0.40210
			ds	0.48116	0.29732	0.40335
	0.60E+00	*vs*	ss	0.46911	0.68557	0.73335
			ds	0.42083	0.65718	0.70823
		0.01	ss	0.46149	0.57397	0.45919
			ds	0.41369	0.55938	0.44249
		0.10	ss	0.40354	0.29214	0.35366
			ds	0.36047	0.29140	0.33551
0.60E+00	0.30E+00	*vs*	ss	0.56882	0.72076	0.83745
			ds	0.56947	0.72420	0.83343
		0.01	ss	0.56007	0.57689	0.52728
			ds	0.56047	0.57919	0.52764
		0.10	ss	0.49082	0.28446	0.41045
			ds	0.49164	0.28503	0.41124
	0.60E+00	*vs*	ss	0.52919	0.57909	0.81905
			ds	0.50056	0.52043	0.80822
		0.01	ss	0.51909	0.47813	0.51853
			ds	0.48962	0.43503	0.51520
		0.10	ss	0.44253	0.25745	0.37875
			ds	0.40993	0.24467	0.36649

example is depicted in Table 4. It is interesting that the frequency ratio for the shorter beam decreases more rapidly than for the longer one, thus, the frequencies of short beams appear to be more sensitive to cracks than those of slender beams, particularly for the first mode. For higher modes this observation may diminish. For slenderness ratios $\bar{s} < 10$, it is

Table 4. Slenderness raio effect for the first five frequency ratios $\Omega_i = (\beta_i/\beta_{iu})^2$ for example 1 of Table 1

	Modal frequency ratio				
$\bar{s}$	Mode I	Mode II	Mode III	Mode IV	Mode V
10	0.6791	0.9176	0.9480	0.9382	0.9442
20	0.7946	0.9448	0.9720	0.9651	0.9615
40	0.8799	0.9661	0.9853	0.9834	0.9762
100	0.9463	0.9842	0.9939	0.9913	0.9888
200	0.9723	0.9916	0.9969	0.9932	0.9941

necessary to use the Timoshenko beam theory in which the rotary inertia and the shear deformation effects should be taken into consideration, in both the equation of motion and the end conditions as well as the continuity and compatibility (Kikidis and Papadopoulos, 1992).

3.3. *Diagnosis capability*

The natural frequencies of the system and mode shapes are considered as the main data required to monitor any machine or structure (Muszynska, 1991). Analytical models of the machine or structure's dynamic behaviour, particularly the model based on a modal approach, are of tremendous value in future diagnostic procedures. The model presented herein is valid to obtain numerical data for stationary beam–mass type structures of important application, such as robot arms (Abramovich and Hamburger, 1992). It is interesting to note that the present model should be modified for rotating beams (rotors) which undoubtedly have different crack models (Gasch, 1993).

From the dynamic point of view, the qualitative charts presented in this work may help the designer to be familiar with the system behaviour in designing suchlike problems. In addition, these charts may be considered as one of the tools required in crack diagnostic procedures. Regarding the first group (Figs 3–12), if the experimental results are carried out and the first few frequencies are known, the identification of crack depth becomes possible by using a suitable technique and the present analysis. Also, for the second group (Fig. 13), both crack location and magnitude may be identified when the experimental frequencies are known.

On the other hand, for mass(es) beam systems, the magnitude and location of an intermediate mass may be detected. One can follow the variation in the modal frequency parameters (Fig. 14) for a typical case of end mass loaded cantilever beam with $\bar{m}_2 = 0.5$ carrying an intermediate mass which moves along the beam length. Four values of intermediate mass ratio are chosen: $\bar{m}_1 = vs$, 0.25, 0.5 and 1.0. As expected, an increase in the mass decreases the frequency ratio; and also, for each specific mode, there is an interesting point at which the frequency becomes minimum.

4. CONCLUSIONS

A modal analysis study of the influence on the system vibration modes of one or two cracks in a uniform prismatic beam elastically restrained against rotation and translation at both ends and carrying lumped masses with rotary inertia is presented. The mathematical formulation of this study is based on the well known Euler–Bernoulli bending theory and

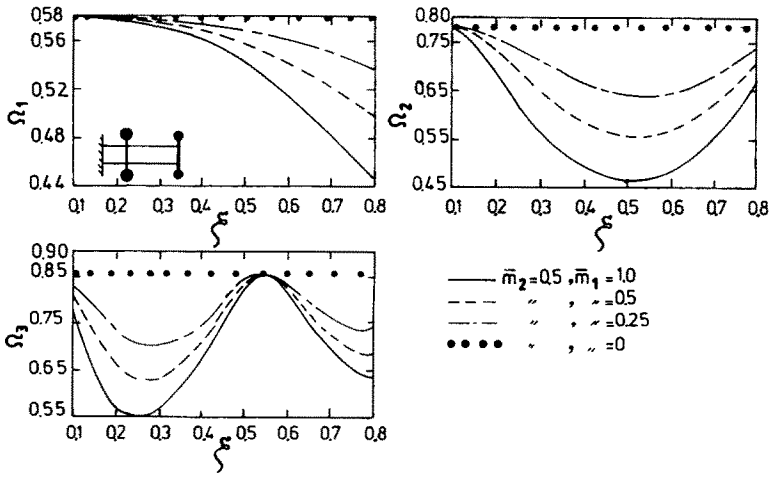

Fig. 14. The variation in the first three modal frequencies for three different intermediate mass ratios, and end mass of $\bar{m}_2 = 0.5$.

freshly derived flexibility polynomials for transverse open cracks. A system frequency equation in a discrete matrix form is derived. Parametric studies are carried out for the effect of stiffness of elastic constraints, the location and magnitude of the cracks, the concentrated masses and the rotary inertia, for the 10 combinations of the well known four classical end conditions, on the natural frequency parameters and mode shapes of the system. Good agreement is found between the results obtained using the derived system frequency equation and those of previous investigators. The present analytical diagnostics permit the user to run the program to analyse the cracked beam system to verify the presence of the crack signature by comparing the test data with analytical predictions. The user would have to judiciously select and try out different locations and depths for the analysis. The present model can be easily extended to the case in which the beam may be attached to more than two concentrated intermediate masses located at positions with or without transverse open cracks. Elastic elements may be added to the intermediate elements for more applicable systems.

REFERENCES

Abramovich, H. and Hamburger, O. (1992). Vibration of a cantilever Timoshenko beam with translational and rotational springs and with a tip mass. *J. Sound Vibration* **157,** 67–80.

Atluri, S. N. (1986) *Computational Methods in the Mechanics of Fracture*. North-Holland, Amsterdam.

Bapat, C. N. and Bapat, C. (1987). Natural frequencies of a beam with non-classical boundary conditions and concentrated masses. *J. Sound Vibration* **112,** 177–182.

Bishop, R. E. D. and Johnson, D. C. (1979). *The Mechanics of Vibration*. Cambridge University Press, Cambridge.

Cawley P. and Adams, R. D. (1979). A vibration technique for non-destructive testing of fibre composite structures. *J. Composite Mater.* **13,** 161–175.

Christides, S. and Barr, A. D. (1984). One-dimensional theory of cracked Bernoulli–Euler beams. *Int. J. Mech. Sci.* **26,** 639–648.

El-Dannanh, E. H. and Farghaly, S. H. (1994). Natural vibrations of cracked shafts carrying elastically mounted end masses. *J. Sound Vibration* (in press).

Farghaly, S. H. (1994). Vibration and stability analysis of Timoshenko beams with discontinuities in cross-section. *J. Sound Vibration* (in press).

Gao, H. and Herrmann, G. (1992). On estimates of stress intensity factors for cracked beams and pipes. *Engng Fracture Mech.* **41,** 695–706.

Gasch, R. (1993). A survey of the dynamic behaviour of a simple rotating shaft with a transverse crack. *J. Sound Vibration* **160,** 313–332.

Gounaris, G. and Dimarogonas, A. D. (1988). Finite element of a cracked prismatic beam for structural analysis. *Computers Structures* **28,** 309–313.

Gudmundson, P. (1984). The dynamic behaviour of slender structures with cross-sectional cracks. *J. Mech. Phys. Solids* **31,** 329–345.

Hamdan, M. N. and Abd-El Latif, L. A. (1992). Analysis of free vibrations of cantilever beams with attached inertia elements using various discretization methods. *Engineering Research Bulletin, Faculty of Engineering and Technology* (MATARIA), Cairo, Egypt. Vol. 2, pp. 183–203.

Haisty, B. S. and Springer, W. T. (1988). A general beam element for use in damage assessment of complex structures. *Trans. Am. Soc. Mech. Eng., J. Vibration, Acoustics, Stress, Reliability in Design* **110,** 389–394.

Hellan, K. (1984) *Introduction to Fracture Mechanics*. McGraw-Hill, New York.

Kikidis, M. L. and Papadopoulos, C. A. (1992). Slenderness ratio effect on cracked beam. *J. Sound Vibration* **155,** 1–11.

Liu, W. H. and Huang, C. C. (1988). Vibrations of a constrained beam carrying a heavy tip body. *J. Sound Vibration* **123,** 15–29.

Muszynska, M. (1991). Rotating machinery malfunction diagnostics through vibration monitoring. *Current Advances in Mechanical Design and Production*, 5th Cairo University MDP Conference, pp. 629–653.

Ostachowicz, W. M. and Krawczuk, M. (1991). Analysis of the effect of cracks on the natural frequencies of a cantilever beam. *J. Sound Vibration* **150,** 191–201.

Petroski, H. J. (1981). Simple static and dynamic models for the cracked elastic beam. *Int. J. Fracture* **17,** R71–R76.

Shen, M. H. H. and Pierre, C. (1990). Natural modes of Bernoulli–Euler beams with symmetric cracks. *J. Sound Vibration* **138,** 115–134.

Srinath, L. S. and Das, Y. C. (1967). Vibrations of beams carrying mass. *Trans. Am. Soc. Mech. Eng., J. Applied Mech.* **34,** 784–785.

APPENDIX: NOMENCLATURE

A	cross section area of the beam
A_i, $i = 1$–12	unknown coefficients
a_i, $i = 1, 2$	parameters defined as in equation (7)
b	width of the beam
d	crack depth

e_1 $= L_1/L$, non-dimensional location parameter of the point 1
e_2 $= L_2/L$, non-dimensional location parameter of the point 2
E Young's modulus of elasticity
h height of the beam section
$\bar{h}$ $= h/L$, inverse of the slenderness ratio $\bar{s}$
I second moment of cross-sectional area
J_1 mass moment of inertia of the mass m_1
$\bar{J}_1$ $= J_1/\rho AL^3$
J_2 mass moment of inertia of the mass m_2
$\bar{J}_2$ $= J_2/\rho AL^3$
$\bar{K}_1$ stiffness of the translational spring at the left end
K_2 stiffness of the translational spring at the right end
L total length of the beam
L_1 length of the beam segment 1
L_2 distance between the second crack location and the left end
m $= \rho AL$, total mass of the beam
m_1 attached mass at the crack location 1
$\bar{m}_1$ $= m_1/m$
m_2 attached mass at the crack location 2
$\bar{m}_2$ $= m_2/m$
$\bar{s}$ slenderness ratio
x distance
y transverse displacement
Z_1 $= K_1L^3/EI$, translational spring rigidity parameter at the left end
Z_2 $= K_2L^3/EI$, translational spring rigidity parameter at the right end
β $= (\rho AL^4\Omega^2/EI)^{0.25}$, frequency parameter
β_i frequency parameter of ith mode for cracked beam
β_{iu} frequency parameter of ith mode for uncracked beam, Table 2
γ_1 $= d_1/h$, crack depth parameter at point 1
γ_2 $= d_2/h$, crack depth parameter at point 2
ζ $= x/L$
θ_1 local flexibility of the crack 1
θ_2 local flexibility of the crack 2
θ_S local flexibility of the single-sided crack
θ_D local flexibility of the double-sided crack
ρ mass density of the beam material
ϕ_1 stiffness of the rotational spring at the left end
Φ_1 $= \phi_1 L/EI$, rotational spring rigidity parameter at the left end
ϕ_2 stiffness of the rotational spring at the right end
Φ_2 $= \phi_2 L/EI$, rotational spring rigidity parameter at the right end
ω_i natural frequency value of the ith mode, Table 2
Ω =circular frequency

Abbreviations

C means clamped (fixed) end
F means free end
P means pinned (hinged) end
S means slide (guided) end
VL $= 100000000$
VS $= 0.00000001$
Y' means $dY/d\zeta$, the first derivative of Y, w.r.t. ζ
Y'' means $d^2Y/d\zeta^2$, the second derivative of Y, w.r.t. ζ
Y''' means $d^3Y/d\zeta^3$, the third derivative of Y, w.r.t. ζ
Y'''' means $d^4Y/d\zeta^4$, the fourth derivative of Y, w.r.t. ζ